Bolocam: a millimeter-wave bolometric camera

Jason Glenn, James J. Bock, Goutam Chattopadhyay, Samantha F. Edgington, Andrew E. Lange, et al.

Jason Glenn, James J. Bock, Goutam Chattopadhyay, Samantha F. Edgington, Andrew E. Lange, Jonas Zmuidzinas, Philip D. Mauskopf, Brooks Rownd, Lunming Yuen, Peter A. R. Ade, "Bolocam: a millimeter-wave bolometric camera," Proc. SPIE 3357, Advanced Technology MMW, Radio, and Terahertz Telescopes, (31 July 1998); doi: 10.1117/12.317418

SPIE.

Event: Astronomical Telescopes and Instrumentation, 1998, Kona, HI, United States

Bolocam: A millimeter-wave bolometric camera

J. Glenn, J. J. Bock, G. Chattopadhyay, S. F. Edgington, A. E. Lange, and J. Zmuidzinas

California Institute of Technology, Mail Code 59-33, Pasadena, CA 91125, USA

P. D. Mauskopf, B. Rownd, and L. Yuen

Five College Radio Astronomy Observatory, Univ. of Massachusetts, Amherst, MA 01003, USA

P. A. R. Ade

Dept. of Physics, Queen Mary and Westfield College, Mile End Road, London E1 4NS, UK

ABSTRACT

We describe the design of Bolocam, a bolometric camera for millimeter-wave observations at the Caltech Submillimeter Observatory. Bolocam will have 144 diffraction-limited detectors operating at 300 mK, an 8 arcminute field of view, and a sky noise limited NEFD of $\sim$ 35 mJy $\mathrm{Hz}^{-\frac{1}{2}}$ per pixel at $\lambda = 1.4$ mm. Observations will be possible at one of $\lambda = 1.1$, 1.4, or 2.1 mm per observing run. The detector array consists of sensitive NTD Ge thermistors bonded to silicon nitride micromesh absorbers patterned on a single wafer of silicon. This is a new technology in millimeter-wave detector array construction. To increase detector packing density, the feed horns will be spaced by $1.26f\lambda$ (at $\lambda = 1.4$ mm), rather than the conventional $2f\lambda$. DC stable read out electronics will enable on-the-fly mapping and drift scanning. We will use Bolocam to map Galactic dust emission, to search for protogalaxies, and to observe the Sunyaev-Zel'dovich effect toward galaxy clusters.

Keywords: bolometers, millimeter-wave

1. INTRODUCTION

Large format millimeter and submillimeter bolometer array cameras are needed to address important problems in astrophysics that require mapping continuum emission from large regions of sky. For example, much of the radiation from stars in young protogalaxies is likely absorbed by dust and reradiated at far infrared wavelengths. This emission will be redshifted to submillimeter and millimeter wavelengths for galaxies at high redshifts ($z \geq 3$). Although this class of galaxies has not been identified, an analysis of the *COBE* FIRAS data indicates a submillimeter background ($\sim$ 3 mJy per square arcminute extrapolated to $\lambda = 1.4$ mm) that could arise from these galaxies.[1] Bolocam will be used to search for protogalaxies, and similarly to search for embedded protostars in cold ($\sim$ 30 K) Galactic molecular cloud cores.

Bolocam will also be optimized for observations of the Sunyaev-Zel'dovich (SZ) effect. The SZ effect is Compton scattering of cosmic microwave background photons by hot gas in galaxy clusters.[2] Observations of the SZ effect combined with x-ray observations can be used to determine the Hubble constant and measure the peculiar velocities of galaxy clusters[3,4] There are two components of the SZ effect: the thermal component and a kinetic component caused by the motion of the cluster with respect to the observer. With observations at $\lambda = 1.1$, 1.4, and 2.1 mm it is possible to separate the kinetic and thermal components.[5] Measurement of the peculiar velocities of a substantial number of galaxy clusters can yield an estimate of the local mass density of the universe through its gravitational effect on the cluster motions.

Several bolometer arrays with increasing numbers of detectors have been constructed in the last several years. This trend toward building imaging cameras is analogous to the evolution of near infrared detectors arrays in the last decade. These instruments include Hertz[6] (the most recent in a series of arrays built by the University of Chicago), SHARC[7,8] and SuZIE[9] at the Caltech Submillimeter Observatory (CSO), a $\lambda = 1.3$ mm array at the IRAM 30

Part of the SPIE Conference on Advanced Technology MMW, Radio, and Terahertz Telescopes
Kona, Hawaii • March 1998 SPIE Vol. 3357 • 0277-786X/98/$10.00

m telescope, and SCUBA[10] at the James Clerk Maxwell Telescope. Bolocam will complement the submillimeter observations of SHARC and SCUBA with millimeter-wave observations.

Bolometer technology has matured dramatically in the last few years resulting in substantial improvements in performance. At the heart of Bolocam will be an array of silicon nitride micromesh bolometers. In Figure 1 we show a single micromesh bolometer. The center of the Si_3N_4 mesh is metallized to form an absorber. The germanium neutron transmutation doped thermistor (20 μm $\times$ 100 μm $\times$ 300 μm) is indium bump bonded to the absorber. Mesh absorbers have several advantages over conventional solid absorbers, including smaller heat capacity, higher resonant vibration frequency (reducing susceptibiliy to microphonics), and lower cross section to cosmic rays. NEPs as low as 1.3×10^{-17} W $Hz^{-\frac{1}{2}}$ have been achieved at a heat sink temperature of 300 mK with a $1/f$ knee below 20 mHz. For Bolocam, the absorbers will all be etched from the same wafer of silicon that will be sandwiched between an array of feed horns and backshorts. This technology is a candidate for use in the SPIRE (Spectral and Photometric Imaging REceiver) bolometer camera of the ESA/NASA *FIRST* mission. Bolocam provides an excellent opportunity to test and improve this technology before flight.

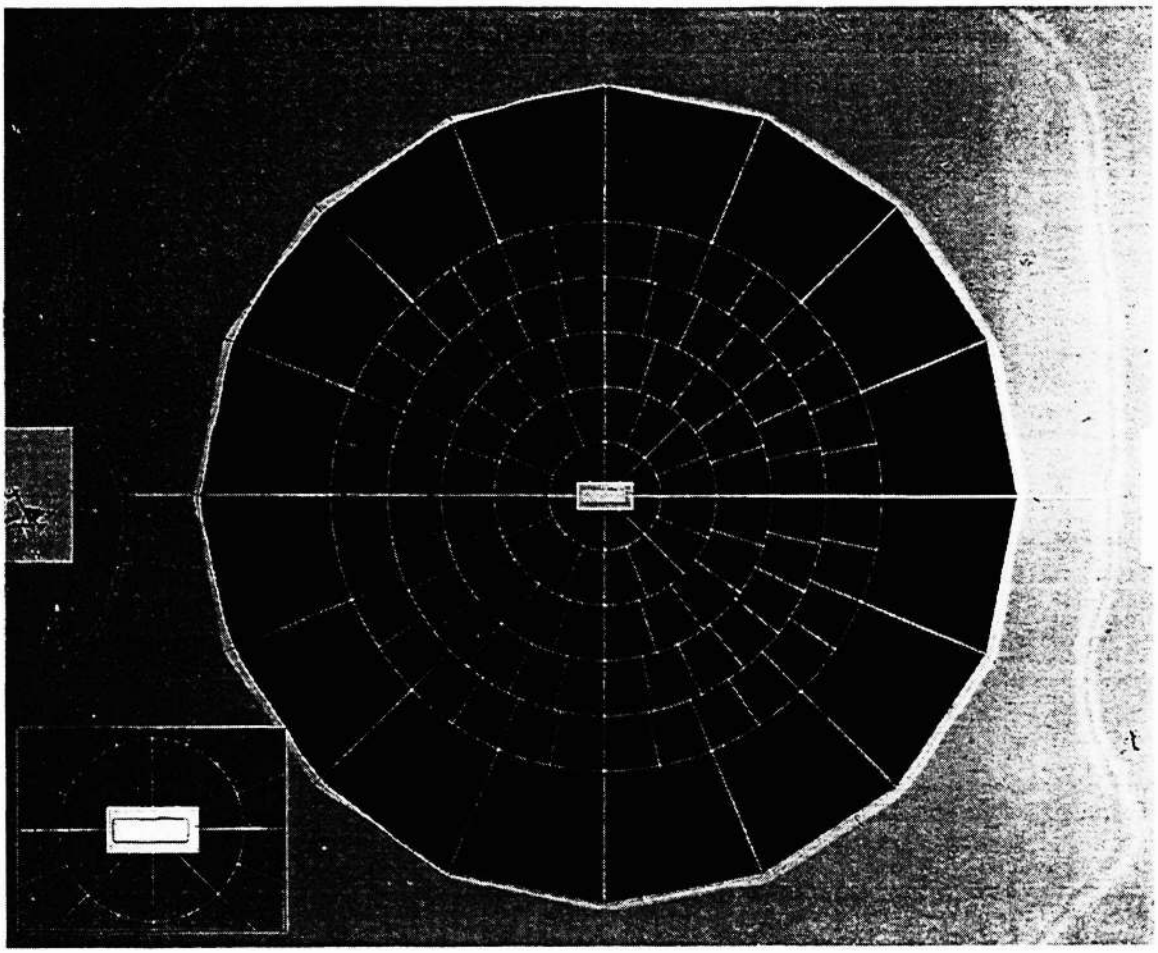

Figure 1. A micromesh bolometer. The thermistor is indium bump bonded to the pad in the center of the absorber. The silicon nitride mesh is made up of legs 1 μm $\times$ 5 μm in cross section and the diameter of the absorber is 5.6 mm. The absorption cross section is the same as a solid absorber of the same area, but the low filling factor reduces the heat capacity and absorption cross section to cosmic rays significantly compared to solid absorbers.

2. DESIGN OVERVIEW

Two versions of Bolocam will be constructed, initially one for the CSO and later one for the 50 m Large Millimeter Telescope (the LMT is a collaboration between the University of Massachussettes and the Instituto Nacional de Astrophysica, Óptica, y Electrónica in Mexico). The CSO is a 10.4 m diameter telescope located atop Mauna Kea in Hawaii. Bolocam will have 144 pixels, an 8 arcminute field of view, and bandpasses at one of $\lambda = 1.1$, 1.4, and 2.1 mm per observing run. The feed horns will illuminate the inner 8.15 m of the primary mirror, yielding a spatial resolution of 43 arcseconds at $\lambda = 1.4$ mm. The bolometers will have a base temperature of 300 mK provided by a sorption refrigerator and a standard liquid nitrogen and liquid helium dewar.

Bolocam will have two observing modes: beam switching and drift scanning/on-the-fly mapping. Since cloud cores and galaxy clusters typically extend a few arcminutes, beam switching will be optimum for observations of these objects. Drift scanning, which will be enabled by a new DC stable total power read-out circuit, will be optimum for mapping areas of sky larger than a few fields of view. In this observing mode, atmospheric emission will be removed by detector differencing in software. Drift scanning will be particularly useful for observations of faint, extended sources since the telescope will be motionless and therefore the sidelobes will not be modulated.

Bolocam has been designed in a modular fashion to keep the focal plane and readout electronics compact. The feed horns and cavities (backshorts) are machined into single pieces of aluminum and invar, respectively. The 300 mK and 120 K bias and readout modules are made commercially with surface mount components mounted on alumina and fiberglass.[11]

3. BOLOMETERS AND INTEGRATING CAVITIES

Considering the optical background loading (see Section 6), we have optimized our bolometers to have NEPs of $\sim 3 \times 10^{-17}$ W Hz$^{-\frac{1}{2}}$ and thermal conductivities to the 300 mK bath of $G = 2 \times 10^{-10}$ W K^{-1}. The 300 mK refrigerator has an intermediate stage at 1.2 K and operates from a 4.2 K cold stage.[12] This eliminates the need to pump on the liquid ^{4}He reservoir.

Figure 2 is a photograph of a prototype bolometer array fabricated at the Center for Space Microelectronics at the Jet Propulsion Laboratory. The silicon wafer is 200 μm thick and 76 mm in diameter with a thin film of Si_3N_4 on top. In the fabrication process, the thermistors are indium bump bonded to the absorbers, then the silicon backing is etched away from the silicon nitride absorber and support legs. Gold leads on two of the support legs (1 μm $\times$ 4.5 μm in cross section) provide the thermal conductivity to the temperature controlled 300 mK bath. The 2.0 mm diameter mesh is metallized to provide a 200 Ω sq^{-1} impedance. Gold is deposited on two of the support legs to bias and read out the bolometers. These leads run to contact pads on the edges of the wafer that will be wire bonded to six standard micro-D-sub connectors with 24 channels each. Mechanical support for the wafer is provided by clipping it to the backshort array. To minimize mechanical stress applied to the wafer during cooling, the integrating cavity array is machined from invar, which has a thermal expansion coefficient very similar to silicon. Thin vespel tubes rigidly suspend the array from the 4.2 K stage and provide the necessary thermal isolation.

The preliminary integrating cavity design is intended to produce constructive interference of the electric field at the absorber by reflection from a backshort. Two adjacent integrating cavities are shown in cross section in Figure 3. In parallel with laboratory measurements, we are using HFSS[13] to simulate and optimize the cavity design and absorber impedance, and to investigate cross talk. It is possible that radiation will leak between cavities by entering the silicon substrate and bouncing between the backshort and feed horn array. Our prelimary simulations of an ideal, monochromatic cavity and absorber suggest that crosstalk will be as little as a few percent. This is because the radiation must make multiple passes through the bolometer before being reflected to adjacent cavities. Crosstalk can be reduced by evaporating an absorbing metal mesh onto the silicon wafer.

4. DETECTOR BIAS AND READOUT

A simplified schematic of a single channel of the DC stable readout circuit is shown in Figure 4. To stay above the $1/f$ noise and eliminate the need to beam switch, the bolometer is AC biased with a square wave at ~ 400 Hz. Low noise NJ132 JFETs[14] decrease the readout line impedance from a few MΩ to 500 Ω. The parallel JFETs and INA 103 instrumentation amplifier[15] provide a common mode rejection ratio of -120 dB to electrical noise pickup. With this configuration, amplifier noise of less than 5 nV$_{rms}$ Hz$^{-\frac{1}{2}}$ has been measured down to 20 mHz. A bandpass filter (16 mHz to 15 Hz) after the lock-in amplifier removes the DC offset from the JFETs and rejects noise at frequencies

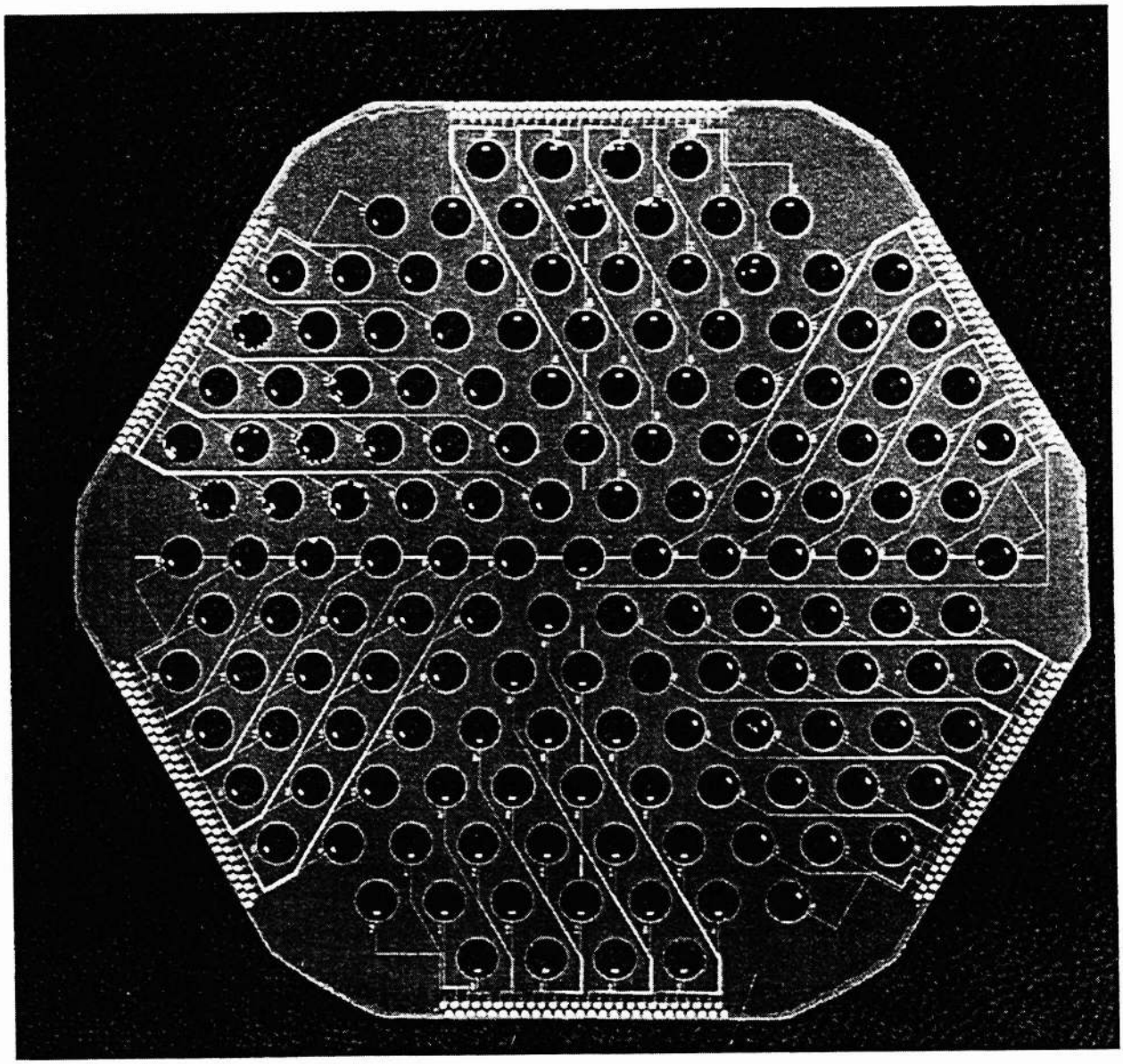

Figure 2. A prototype Bolocam bolometer array. The absorbers are 2.0 mm in diameter and the wafer is 200 μm thick. The support legs are 0.5 mm × 4.5 μm × 1 μm, the web legs are 165 μm × 4 μm × 1 μm, and the filling factor is 4.5%. The thermistor pads are offset from the center of the absorbers. Gold traces connect the bolometers to the wire bond pads at the edges of the wafer.

above the fastest sampling frequency. Digitization and recording of the data will be done with CSO facility 16-bit A/Ds and computers.

Because there are 144 bias and readout channels that conduct heat from the dewar vacuum shield, the wiring has been considered carefully. The micro-D-sub connectors bonded to the wafer plug into commercially manufactured load resistor array modules. The bolometers are connected to the 1.2 K stage and then to the JFET modules by cryogenic cable. The cables consist of 24 twisted pairs of 0.003 inch manganin wires woven into ribbon cables. They extend for 10 cm between 300 mK and 4.2 K, producing a heat load of less than 18 μW for all six cables. A 10 cm length of cable between the 4.2 K stage and the $\sim$ 120 K stage should produce a heat load of less than 30 mW to the

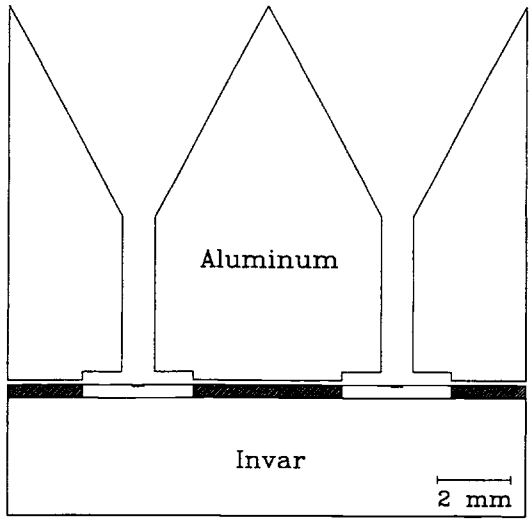

Figure 3. A cross section of two adjacent $\lambda = 1.4$ mm integrating cavities we are simulating and testing in the laboratory. The feed horns have been shortened by a factor of ~ 3 for display. The distance between the top of the cavities and the absorbers is $\lambda/4$ and the distance between the absorbers and the backshort is $\lambda/4$. The hatched region is silicon. Because the bolometer array is fragile, the backshort, which contacts the array, will be machined from invar to nearly match the thermal expansion coefficient of the silicon.

liquid helium for all six cables. Cables of this construction also carry the output signals to the connectors on the room temperature vacuum shell. Based on our heat loading calculations and the liquid helium consumption rate of a dewar with a single readout (and no vacuum window), we expect a liquid helium consumption of less than 0.2 liters per hour.

The JFETs are mounted on alumina substrates and placed in a radiation-shielded box (heat sunk to 4.2 K) behind the bolometer array. The JFET modules are suspended from the liquid helium temperature work surface by insulating G-10 fiberglass legs. They are heat sunk to the 77 K LN_2 reservoir by a 0.25 inch copper rod that extends through a hole in the center of the liquid helium reservoir. They will self heat to near the optimum operating temperature of ~ 120 K, which will be controlled precisely with a heater.

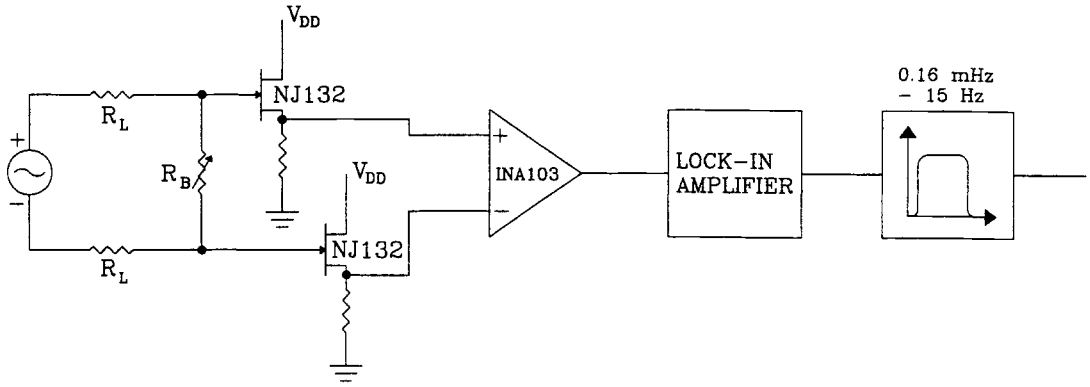

Figure 4. A simplified schematic of the DC stable readout circuit. Bolocam will have 144 identical readout channels. The 400 Hz square wave bias voltage eliminates the need to beam switch to modulate the bolometer above the $1/f$ noise. With the offset removed by the filter, the output is proportional to the total power incident on the bolometer. CSO facility 16-bit A/D converters and computers will record the data.

5. OPTICAL DESIGN

The Bolocam optics consist of a set of reimaging mirrors outside of the dewar and the cold optics shown schematically in Figure 5. The Cassegrain focus is reimaged onto the focal plane by the mirrors and a high density polyethylene lens. We have not finalized the design of the warm relay optics yet, however the most likely configuration is simply two folding flats and an ellipsoidal mirror. The ellipsoidal mirror converts the f/12.36 Cassegrain beam to f/7.5 at the dewar window. With this configuration, we are able to achieve Strehl ratios of 0.97 or better at $\lambda = 1.1$ mm over the entire field of view on axis. Since atmospheric emission will be removed by differencing pixels in the drift scanning mode, the design is also being optimized to give maximum overlap of the beams on the primary mirror (and therefore through the atmosphere). With our preliminary design, the maximum deviation of the centroid of any beam from the center of the primary mirror is 0.5 m.

To minimize beam spillover beyond the primary and secondary mirrors, the primary mirror is reimaged onto a Lyot stop. Only rays that strike the inner 8.15 m of the primary mirror propagate through the Lyot stop onto the focal plane. The lens brings the beam to a focus at the feed horns with a final plate scale of 35 arcseconds per horn. The distance from the Lyot stop to the lens is exactly the focal length of the lens, placing the image of the Lyot stop at infinity as viewed from the feed horns. This makes the focal plane nearly flat and ensures the beams from all the feed horns are truncated nearly identically by the Lyot stop.

We favored feed horns and integrating cavities over bare detectors because horns and cavities provide immunity to stray radiation and, in practice, higher optical efficiency. To allow us to pack more detectors in a small focal plane, we chose feed horns with $1.26f\lambda$ entrance aperture diameters (and therefore $1.26f\lambda$ center-to-center spacing in the hexagonal pack) rather than the conventional $2f\lambda$ diameters. With $1.26f\lambda$ spacing, Nyquist sampling can be achieved with two drift scans or four jitter positions. The primary objection to $1.26f\lambda$ spacing is that the aperture efficiency is reduced to 0.57 from 0.78 for $2f\lambda$ horns. For a given number of detectors, if the region to be mapped is signficantly larger than the field of view, $2f\lambda$ horns are superior because the mapping speed per detector is greater. However, mapping a small region to a target signal to noise ratio searching for point sources under sky noise limited observing conditions takes approximately twice as long for $2f\lambda$ spacing as for $f\lambda$ spacing.[16]

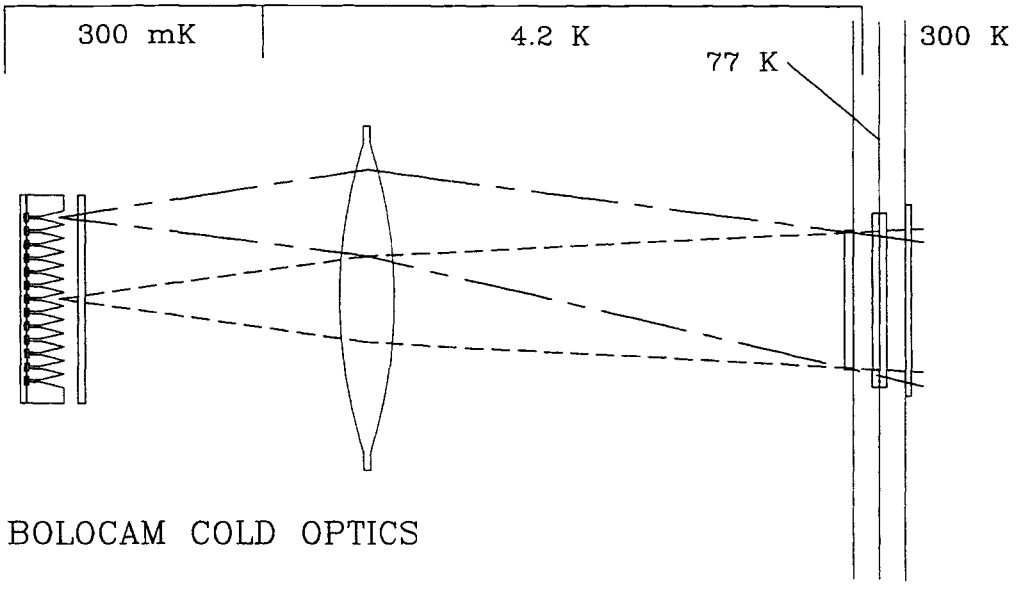

Figure 5. The cold Bolocam optics. Rays converging from the warm reimaging optics are shown for the center and one edge of the field of view. A light tight radiation shield heat sunk to 4.2 K encloses the JFETs which are heat sunk to 77 K and will self heat to 120 K. The filters are described in the text. The lens is high density polyethylene with antireflection grooves.

Propagating a single-mode gaussian beam from the conical feed horn at the center of the array indicates that the beams will be apodized at approximately -2.7 dB by the Lyot stop. With this edge taper, approximately 55% of the power from each horn is intercepted by the 4 K Lyot stop. The low edge taper is a consequence of using $1.26f\lambda$ feed horns. Even with a very small flare angle (i.e., $\sim 8°$ semi-flare angle), the edge taper cannot be decreased significantly. Ignoring the beam broadening caused by the small edge taper at the Lyot stop, the secondary and primary mirrors will be illuminated with a -2.7 dB edge taper at their 80% radius contour.

Bolocam will have three bandpasses centered on $\lambda = 1.1$, 1.4, and 2.1 mm, but only one bandpass will be available per observing run. Between observing runs, the 300 mK filter and feedhorn/waveguide array will be replaced to provide one of the other two bandpasses. This choice was made over a cold filter wheel to simplify the focal plane assembly and minimize susceptibility to light leaks.

The filtering system includes optical and infrared blockers and resonant metal mesh filters. Starting at 300 K, there is a high density polyethylene vacuum window tuned for constructive interference in transmission at the observation wavelength. At the 77 K window a quartz filter antireflection coated with black polyethylene provides infrared blocking. This is followed by a metal mesh 10 cm^{-1} low pass filter. A glass filter rejects far infrared radiation at the 4 K cold stop. A 7.67 cm^{-1} metal mesh filter at 300 mK in front of the feed horns forms the high frequency edge of the bandpass. The waveguides define the low frequency edge of the bandpass for each band.

6. SENSITIVITY

We estimate the sensitivity of Bolocam by scaling the sensitivity obtained with SuZIE drift scan observations. This comparison is relevant because the instruments operate in the same wavebands and are dominated by sky temperature fluctuations. The main differences between BOLOCAM and SuZIE are 1) the beam size/throughput of each pixel, 2) the angular separation between pixels, 3) the effective modulation speed of the observation, and 4) the number of pixels. BOLOCAM has 1/8 the throughput per pixel of the SuZIE 1.5 system. The amplitude of atmospheric emission fluctuations in a single pixel is proportional to the throughput and therefore will be smaller by a factor of 1/8 for Bolocam than for SuZIE. The effective modulation frequency of a BOLOCAM drift scan is three times higher than the modulation frequency in a SuZIE drift scan since the beam size is three times smaller. The measured power spectrum of atmospheric fluctuations in SuZIE observations is proportional to $f^{-1/3}$, so the amplitude of sky noise will be reduced by a factor of $3^{1/3} \simeq 1.4$.

We expect to gain an additional factor of ~ 3 improvement in sensitivity to point sources by removing the sky emission that is correlated across the array. First, we can remove the common mode signal from the array without significantly increasing the noise in any one pixel because we can average across the array. In constrast, the electronic differencing adds a factor of $\sqrt{2}$ to the noise with SuZIE observations. Second, we expect an additional factor of two improvement in differential noise because the Bolocam beams are 5.5 times closer together on the sky than the SuZIE beams, and therefore probe more similar columns of atmosphere.

SuZIE 1.5 has a point source sensitivity of $\simeq 1$ Jy/ $\mathrm{Hz}^{-\frac{1}{2}}$ at $\lambda = 1.1$ mm in good weather at the CSO. Including all of the above factors, we expect the sensitivity of BOLOCAM at 1.1 mm will be limited by sky temperature fluctuations at a level:

$$\mathrm{NEFD_{sky}} = 1 \text{ Jy Hz}^{-\frac{1}{2}} \cdot \left(\frac{A\Omega_{\mathrm{BC}}}{A\Omega_{\mathrm{SZ}}}\right)\left(\frac{\theta_{\mathrm{BC}}}{\theta_{\mathrm{SZ}}}\right)^{1/3} \cdot \frac{1}{3} = 30 \text{ mJy Hz}^{-\frac{1}{2}}. \quad (1)$$

If we assume that the atmospheric emission is in the Rayleigh-Jeans limit and is proportional to ν^2, the contribution to the NEFD is wavelength independent because the improvement of atmosphere at the longer wavelengths is offset by the increase in the beam solid angles. Since the atmospheric noise does decline more rapidly than ν^2, $\mathrm{NEFD_{sky}}$ will be less than 30 mJy $\mathrm{Hz}^{-\frac{1}{2}}$ at $\lambda = 1.4$ and 2.1 mm.

The detector noise and background limited photon noise (BLIP) are determined by loading from telescope emission and the optical efficiency. We have consistently measured a telescope emission of 30 K and an atmospheric emission of about 10 K with SuZIE at the CSO. With an efficiency (filter optical efficiency $\times$ fractional reduction in throughput by the Lyot stop) of $\eta = 0.2$ at $\lambda = 1.1$ mm, the expected optical loading on each detector in Bolocam is 8 pW. A reasonable bolometer NEP for this loading is 3×10^{-17} W $\mathrm{Hz}^{-\frac{1}{2}}$. Filling 52 m^2 of the CSO over a 38 GHz bandwidth

($\Delta\nu/\nu$ ~0.14 for all three bands) this yields a detector noise contribution to the NEFD of

$$\mathrm{NEFD_{det}} = \frac{3 \times 10^{-17}\ \mathrm{W\ Hz^{-\frac{1}{2}}}}{52\ \mathrm{m^2}\ \Delta\nu\ \eta} = 6\ \mathrm{mJy\ Hz^{-\frac{1}{2}}}. \quad (2)$$

The BLIP noise is:

$$\mathrm{NEP_{BLIP}} \simeq \sqrt{2 P_{opt} h\nu} = 6 \times 10^{-17}\ \mathrm{W\ Hz^{-\frac{1}{2}}} \quad (3)$$

which yields

$$\mathrm{NEFD_{BLIP}} = 9\ \mathrm{mJy\ Hz^{-\frac{1}{2}}}. \quad (4)$$

Since the feed horn entrance aperture diameters will be 5 mm for all three bands, the horn aperture efficiencies and throughput through the Lyot stop decrease from λ = 1.1 to 1.4 to 2.1 mm. In combination with the smaller bandpasses at longer wavelengths, this increases the BLIP and detector NEFDs at the longer wavelengths. Table 1 lists beam sizes and estimated sensitivities (rounded to the nearest 5 mJy $\mathrm{Hz^{-\frac{1}{2}}}$) derived from adding the detector, BLIP, and sky emission NEFDs in quadrature for the three wavebands. Since the sky noise is likely overestimated in the 1.4 and 2.1 mm bands, the actual NEFDs should be smaller than those listed in the table and BLIP and detector noise will dominate at 2.1 mm.

Band mm	θ_{FWHM} arcsec	$\mathrm{NEFD_{per\ pixel}}$ mJy $\mathrm{Hz^{-\frac{1}{2}}}$
1.1	34	30
1.4	43	35
2.1	65	45

7. CONCLUSION

In this paper we described the design of Bolocam, a millimeter-wave bolometer camera for use at the Caltech Submillimeter Observatory. Bolocam will have 144 bolometers bonded to closely-packed absorbers etched from a single silicon wafer. This represents a new technology in millimeter-wave detector array construction. Bolocam will have DC stable readouts so it will be possible to drift scan, eliminating the need for beam switching to modulate the bolometers above the $1/f$ noise. With the expected NEFD of ~ 35 mJy $\mathrm{Hz^{-\frac{1}{2}}}$ per pixel at λ = 1.4 mm and a field of view of 8 arcminutes, it will be possible to map one half of a square degree of sky to an rms sensitivity of ~ 1 mJy in just less than 30 hours of integration. The design of Bolocam is nearly complete and subsystems are under construction and testing.

ACKNOWLEDGMENTS

We thank Tom Phillips, Gene Serabyn, and Luca Olmi for useful discussions regarding the design of the Bolocam optics. We thank Matt Griffin and Walter Gear for discussions regarding mapping speed as a function of feed horn spacing. The construction of Bolocam is funded by a JPL President's Fund grant to P. Mauskopf and J. J. Bock, by the Large Millimeter Telescope project, and by NASA through the Advanced Technology Program. The Caltech Submillimeter Observatory is operated by Caltech under a grant from the National Science Foundation.

REFERENCES

1. Puget, J.L., Abergel, A., Bernard, J.P., Boulanger, F., Burton, W.B., Desert, F.- X., and Hartmann, D., "Tentative Detection of a Cosmic Far-Infrared Background With COBE", *Astron. and Astrop.*, **308**, pp. L5-L8.
2. Sunyaev, R.A. and Zel'dovich, Y.B., "Microwave Background Radiation As a Probe of the Contemporary Structure and History of the Universe", *Ann. Rev. of Astron. and Astrop.*, **18**, pp. 537-560, 1980.
3. Holzapfel, W.L., Arnaud, M., Ade, P.A.R., Church, S.E., Fischer, M.L., Mauskopf, P.D., Rephaeli, Y., Wilbanks, T.M., and Lange, A.E., "Measurement of the Hubble Constant from X-ray and 2.1 mm Observations of Abell 2163", *Astrop. Jour.*, **480**, pp. 449-465, 1997.
4. Holzapfel, W.L., Ade, P.A.R., Church, S.E., Mauskopf, P.D., Rephaeli, Y., Wilbanks, T.M., and Lange, A.E., "Limits On the Peculiar Velocities of Two Distant Clusters Using the Kinematic Sunyaev-Zeldovich Effect", *Astrop. Jour.*, **481**, pp. 35-48, 1997.

5. Fischer, M.L. and Lange, A.E., "Confusion Limits to the Measurement of the Sunyaev-Zeldovich Effects in Clusters of Galaxies at Millimeter Wavelengths", *Astrop. Jour.*, **419**, pp. 433-439, 1993.
6. Dowell, C.D., Hildebrand, R.H., Schleuning, D.A., Vaillancourt, J., Dotson, J.L., Novak, G., Renbarger, T., and Houde, M., "Submillimeter Array Polarimetry with Hertz", *Astrop. Jour*, in press, 1998.
7. Wang, N., Hunter, T.R., Benford, D.J., Serabyn, E., Phillips, T.G., Moseley, S.H., Boyce, K., Szymkowiak, A., Allen, C., Mott, B., and, Gygax, J., "Characterization of a submillimeter high-angular-resolution camera with a monolithic silicon bolometer array for the Caltech Submillimeter Observatory", *Appl. Opt.*, **35**, No. 4, pp. 6629-6640, 1996.
8. Hunter, T.R, Benford, D.J., and Serabyn, E., "Optical Design of the Submillimeter High Angular Resolution Camera (SHARC)", *Publ. of the Astron. Soc. of the Pacific*, **108**, pp. 1042-1050, 1996.
9. Holzapfel, W.L., Wilbanks, T.M., Ade, P.A.R., Church, S.E., Fischer, M.L., Mauskopf, P.D., Osgood, D.E., and Lange, A.E., "The Sunyaev-Zel'dovich Infrared Experiment: a Millimeter-Wave Receiver for Cluster Cosmology", *Astrop. Jour.*, **479**, pp. 17-30, 1997.
10. Cunningham, C.R., Gear, W.K., Duncan, W.D., Hastings, P.R., and Holland, W.S., "SCUBA: The Submillimeter Common-User Bolometer Array for the James Clerk Maxwell Telescope", *Proc. SPIE Symp. on Instrumentation in Astronomy VIII*, **2198**, pp. 638-649, 1994.
11. Sunbelt Microelectronics, 237 Enterprise Road, Deltona, FL 32725-8001
12. Chase Research, 35 Wostenholm Road, Sheffield, S7 1LB, UK
13. High Frequency Structure Simulator, Hewlett-Packard Company, Test and Measurement Organization, P.O. Box 50637, Palo Alto, CA 94303-9512
14. InterFET Corporation, 2000 North Shiloh Road, Garland, TX 75042
15. Burr-Brown Corporation, P. O. Box 11400, Tucson, AZ 85734
16. Bock, J.J., Grannan, S.M., LeDuc, H.G., Turner, A.D., Glenn, J., Lange, A.E., and Irwin, K., "Silicon nitride micromesh bolometer arrays for SPIRE", these proceedings.